



Semnan University

# Mechanics of Advanced Composite Structures

journal homepage: <http://MACS.journals.semnan.ac.ir>

## Synthesis and Characterization Al<sub>2</sub>O<sub>3</sub>/Novolac/Fiberglass Nanocomposite: Modification of Thermal Stability and Thermal Insulation Properties

M. Rezaei Qazviniha, F. Piri\*

Department of Chemistry, Faculty of Sciences, Zanjan University, Zanjan, Iran

### KEYWORDS

Novolac resin;  
Alumina;  
Nanocomposite;  
Thermal insulation;  
Thermal stability.

### ABSTRACT

Alumina (Al<sub>2</sub>O<sub>3</sub>) nanoparticles were used as the additive for modifying a novolac phenolic resin using the solution mixing method. Different weight percentages of nano alumina 3 and 8 w% were loaded into the resin, called 3ARC and 8ARC nanocomposites, respectively. These nanocomposites were investigated by field emission scanning electron microscopy (FE-SEM), X-ray fluorescence spectroscopy (XRF), energy-dispersive X-ray spectroscopy (EDS), and oxyacetylene flame test (OFT). The FE-SEM images exhibited that at low concentrations (3ARC), the nano alumina particles were dispersed uniformly on the surface of novolac resin; however, at high concentrations, the dispersion was repressed by aggregation in the nanocomposites. OFT proved that with increasing alumina content in the nanocomposite, the back temperature of the sample decreases and thus improves the thermal insulation properties.

### 1. Introduction

In recent years, much attention has been paid to new and improved polymers to produce numerous new products [1]. The properties of a polymer can be changed by changing the arrangement of the monomers or the reaction conditions [1]. Phenolic resins (PR) are one of the oldest thermosetting resins that, despite more than one hundred years of their life, still have significant applications in the manufacture of adhesives, coatings, industrial insulation, printed circuits boards, heat shields, and advanced composites [2, 3]. The distinctive feature of these resins is the ease of processing, low cost, and good mechanical properties [3]. PRs are prepared by the reaction of phenol or its derivatives with aldehydes in the presence of a catalyst. Depending on the molar ratio of phenol to formaldehyde and the acidity or alkalinity of the catalyst, the resulting resin can be resol or novolac [4]. Novolac is a phenol-formaldehyde resin with a formaldehyde to phenol molar ratio of less than one. The thermal instability, poor resistance, and inherent brittleness to crack

initiation and growth are disadvantages of pure PRs. In order to be used in engineering applications, their structure must be modified to realize the possibilities of new polymers [5-7]. The most common methods of structural modification of phenolic resins are the use of reinforcements or fillers into a polymer matrix, which is called composite.

Nanocomposites are very interesting because of their potential applications in electromagnetics, electronics, catalysis and nonlinear optics, thermal conducting materials, etc. [8]. One of the most attractive and challenging research areas in the nanocomposites field is nanocomposites of polymer/ceramic and metal fillers, which are usually prepared by mixing nanoparticles of ceramic or metal fillers with a polymer [9].

To increase the thermal stability and conductivity of polymers, a lot of ceramic and metal fillers are used. Metal phases such as Cu, Ni, Al, and Ag [10,11] and ceramic materials such as AlN, Si<sub>3</sub>N<sub>4</sub>, BN, and SiC [12-14] have been used as potential fillers to improve the thermal stability

\* Corresponding author. Tel.: +98-2433052580; Fax: +98-2432282477  
E-mail address: [farideh.piri@znu.ac.ir](mailto:farideh.piri@znu.ac.ir)

of the pure polymer. The ceramics like aluminum nitride, alumina, and silica as fillers have been considered first in electronic packaging [15-17].

Alumina is one of the most attractive ceramics used in various industries as catalyst support, refractory, and abrasive, because of its attractive thermal, mechanical, and chemical properties [18-23]. Many researchers pay special attention to nano alumina as a filler in polymer nanocomposites due to its interesting properties and low cost at the nanoscale relative to nanoparticles such as carbon nanotubes. Therefore, much research has been done to use alumina nanoparticles in polymer matrices to investigate the relationship between structure and properties in nanocomposites [24-31]. In a report, Omrani et al. investigated the effect of nano alumina in the epoxy resin matrix. They found that a low filler concentration improved mechanical and thermal properties [29]. However, Shukla et al. showed that the epoxy matrix with modified alumina platelets as reinforcement had no significant effect on fracture toughness and elastic modulus [32]. Furthermore, the incorporation of 20 vol% alumina nanoparticles in poly(methyl methacrylate) (PMMA) led to the hardness of 101 Shore D, a flexural strength of 129 MPa, and impact energy of 2 kJ/m<sup>2</sup> for the nanocomposite [30]. In other research, the dynamic impact response of carbon fiber/epoxy nanocomposite was significantly improved by the addition of alumina nanoparticles [33].

Nowadays, alumina/novolac/fiberglass composites are used in the aerospace industries as thermal insulators at very high temperatures (above 2000°C) and in the electronics industry as a substrate for electronic boards. To improve the thermal insulation properties of this resin, various methods are used, such as the use of metal oxide nanoparticles, the use of nanoporous materials, and the use of possible molecular methods to change the molecular structure of novolac.

Herein, we investigate the effect of nanofillers Al<sub>2</sub>O<sub>3</sub> on thermal insulation properties of novolac type phenolic resin. The alumina/novolac/fiberglass nanocomposites were prepared by various contents of alumina containing 3 and 8 w% in novolac resin, from now on, called 3ARC and 8ARC. The 0ARC composite is novolac resin without nano alumina, which is synthesized as a control composite. This study aims to maintain or improve the physical-mechanical properties of novolac resin using various methods, to improve the thermal insulation properties of this resin, and to maintain its properties at high temperatures.

## 2. Experimental

### 2.1. Materials

Novolac resin (Industry and Chemical Co., Iran), micro alumina (Nabaltec Co., Germany), 3-(trimethoxysilyl)-propylamine (Sigma Aldrich Co., United States), fiberglass (SP Systems Co., South Korea), dibutyl phthalate (DBP) and Al<sub>2</sub>O<sub>3</sub> nanoparticles (gamma phase, 20 nm, US Research Nanomaterials, Inc.) were used as raw materials to prepare nanocomposites. All starting materials were purchased from commercial sources and were used without further purification.

### 2.2. Preparation of Alumina nanoparticle/Novolac resin/Fiberglass composite

Novolac phenolic resin (159 g) was dissolved in 255 ml ethanol under stirring for one h. Then, micro alumina (15.9 g), DBP (15.9 g), and 3-(trimethoxysilyl)-propylamine (3.75 g) were added to the solution to give a brown solution. To the resin suspension mixture, different amounts of alumina nanoparticles (3 and 8 g) were added and stirred mechanically with a stirrer, followed by sonication to obtain a homogeneous mixture and to break up the agglomerates. Finally, the Al<sub>2</sub>O<sub>3</sub> nanoparticles/Novolac resin mixture was spread evenly on the fiberglass (the fiberglass was treated with an aqueous silane mixture and dried before use) and cured at 157 °C under the pressure of 20 bar for one h. The samples are called nanocomposite without alumina (control sample, 0ARC), nanocomposite containing 3 g of alumina (3ARC), and nanocomposite containing 8 g of alumina (8ARC).

### 2.3. Characterization

The nanostructure of the alumina/novolac/fiberglass composites was detected by a high-resolution field emission scanning electron microscope (FE-SEM) equipped with energy dispersive X-ray analysis (Mira 3-XMU, Czech Republic). Alumina/novolac/fiberglass composites with different alumina contents were characterized with X-ray fluorescence spectroscopy (ARL™ PERFORM'X Sequential). ASTM E 285 was used as a standard test method for oxyacetylene ablation testing of thermal insulation material.

## 3. Results and Discussion

The field emission scanning electron microscopy (FE-SEM) images and energy-dispersive X-ray spectroscopy (EDS) spectra of pure novolac resin (0ARC), 3ARC, and 8ARC nanocomposites before and after the

oxyacetylene flame test (OFT) are shown in Figures 1-3. Figures 1-a and 1-b indicate that the fracture surface of pure novolac (0ARC) was pretty smooth. This demonstrates that 0ARC is typically a brittle material and no monomer intercalation occurred [34]. As seen in the images after the flame test with a temperature of 3000°C, the structure of the novolac resin is destroyed and the porous matrix of fiberglass plus metal oxide particles make up most of the sample (Figures 1-3).

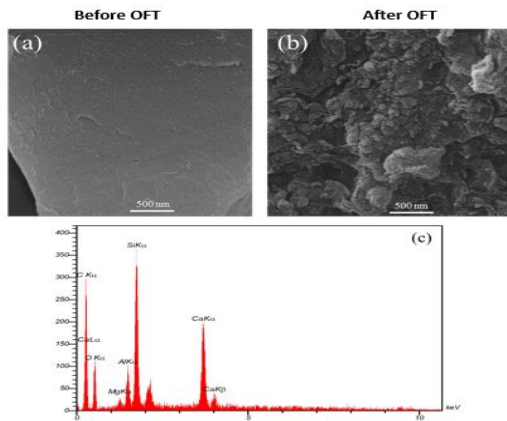


**Fig 1.** The FE-SEM morphologies before and after OFT (a and b) and EDS pattern after OFT (c) of the surface of the 0ARC.

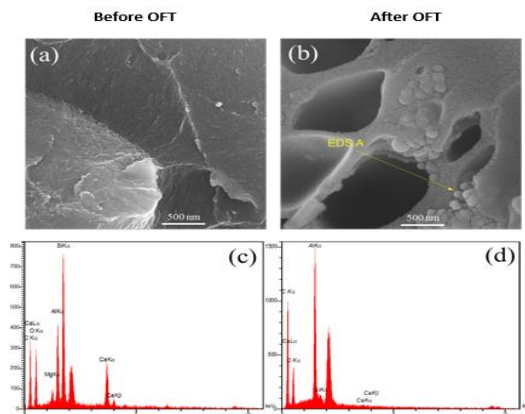


**Fig 2.** The FE-SEM morphologies and EDS patterns of surfaces of 3ARC before (a and c) and after OFT (b and d).

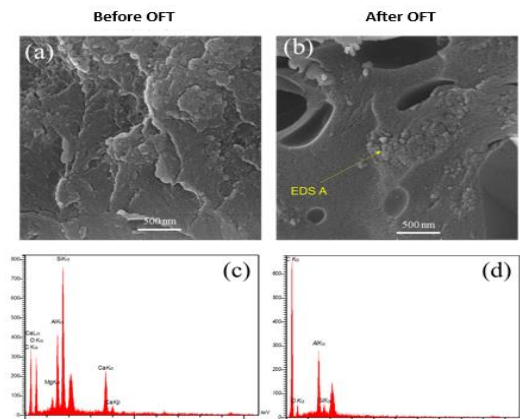


**Fig 3.** The FE-SEM morphologies and EDS patterns of surfaces of 8ARC before (a and c) and after OFT (b and d).

Moreover, in the general view, in the images after the flame test, the presence of a spherical and hollow surface on the surface of the samples can be seen, indicating the creation of a char layer from burning on the sample and the creation of a heat shield caused by this layer. This factor contributes significantly to the insulating property of the sample. The spherical alumina nanoparticles are also well visible on the fiberglass surface in Figures 2-b and 3-b. However, aggregation occurs at high alumina concentrations (8 w%) in the nanocomposite, as shown in Figure 3-b.

Figures 2(c,d), 3(c,d), and Tables 1 and 2 show EDS patterns and values of elements, for the points identified with arrows in FE-SEM images from nanocomposites 3ARC and 8ARC after OFT. These elemental analyzes confirm the presence of alumina nanoparticles in the 3ARC and 8ARC nanocomposite. The comparison of the values related to the percentage of presence of elements before and after the flame test for 3ARC and 8ARC nanocomposites are summarized in Tables 1 and 2. The results clearly show that when the samples are exposed to flame, due to the combustion process, a significant part of the non-carbon elements is removed from the composition and carbon remains as soot on the surface of the sample. As can be seen in these Tables, the percentage of carbon after the flame test has increased by about 20 and 35% for 3ARC and 8ARC, respectively.

The chemical composition of the nanocomposites was analyzed through X-ray fluorescence spectroscopy (XRF). The XRF elemental analysis data of pure novolac (without alumina, 0ARC), alumina/novolac/fiberglass nanocomposites 3ARC and 8ARC before and after OFT are summarized in Table 3.

The results show that the nanocomposites are mainly composed of silicium in the form of silicon dioxide ( $\text{SiO}_2$ ), which represents more than 35 w%. The alumina content in 0ARC is 10.4 w%, which is attributed to the alumina amount in fiberglass. The alumina content increases to 13.79 and 16.7 w% by increasing its amount in 3ARC and 8ARC nanocomposites, respectively. The oxides such as MgO and  $\text{Fe}_2\text{O}_3$  appear with lower percentages, around 2%, and the rest are in amounts less than 1%. Furthermore, oxidation of the polymeric matrix, which occurs in the presence of oxides such as  $\text{Fe}_2\text{O}_3$ , reduces in concentrations below 2 w% [34].

Because the combustion process takes place at a high temperature for novolac resin, the carbon layer forms a heat shield on the surface of the sample.

**Table 1.** The EDS quantitative results of 3ARC

	Element	W%		A%	
		Before OFT	After OFT	Before OFT	After OFT
3ARC	C	68.22	89.87	75.44	92.37
	O	26.86	9.61	22.3	7.42
	Al	2.09	0.81	1.03	0.08
	Si	2.04	0.25	0.97	0.11
	Ca	0.8	0.09	0.26	0.03

**Table 2.** The EDS quantitative results of 8ARC

	Element	W%		A%	
		Before OFT	After OFT	Before OFT	After OFT
8ARC	C	47.15	82.85	59.57	87.73
	O	31.16	11.42	29.55	9.17
	Al	5.08	4.63	2.85	2.60
	Si	9.89	1.10	5.34	0.50
	Ca	6.15	0.0	2.33	0.0

**Table 3.** The chemical composition of 0ARC, 3ARC, and 8ARC nanocomposites

		MgO	Al <sub>2</sub> O <sub>3</sub>	SiO <sub>2</sub>	P <sub>2</sub> O <sub>5</sub>	K <sub>2</sub> O	CaO	TiO <sub>2</sub>	Fe <sub>2</sub> O <sub>3</sub>	Cl
0ARC	Before OFT	1.4	12.3	43.23	0.1	0.24	24.9	0.94	1.2	0.17
	After OFT	1.2	10.4	36.75	0.19	0.26	26.7	1.1	2.1	0.36
3ARC	Before OFT	2.5	14.1	39.11	0.11	0.44	22.5	1.0	1.9	0.32
	After OFT	2.4	13.79	39.2	0.13	0.42	22.0	1.1	1.7	0.3
8ARC	Before OFT	2.2	18.7	37.1	0.1	0.38	19.5	0.85	1.5	0.3
	After OFT	2.1	16.7	35.9	0.15	0.4	20.5	1.2	3.3	0.35

In FE-SEM analysis, carbon is the predominant compound due to the photography and analysis of the sample surface. However, in XRF analysis, because this analysis is performed in the depth of the sample and the matrix material of the samples is fiberglass; therefore, the predominant compound is silicon dioxide.

Furthermore, flame testing and burning of the samples at a temperature of about 2500 °C causes the decomposition of all organic compounds in the samples, and minerals are completely converted to their oxidized form. Compounds such as nitrates, sulfates, and other salts of mineral elements are also removed and only their oxidized form will be present in the samples after the flame test. As can be seen in Tables 1-3, a decreasing trend in the percentage of metal elements and oxides can be seen after the flame test, in which FE-SEM and XRF confirm the increase in the rate of carbon on the surface of the samples and the formation of oxides of new elements in the structure of the samples, respectively.

The OFT was performed on the prepared samples to study the thermal behavior and ablation performance. The flame heat flux was 15000 W/m<sup>2</sup> and after placing the samples at a distance of 8 mm from the tip of the flame, the temperature behind the samples was measured over time. Figure 4 shows the flame test results and a temperature curve as a function of time. The temperature distribution of the back surface of 0ARC, 3ARC, and 8ARC nanocomposites, after 60 seconds of testing, is 861, 730, and 340 °C, respectively. As can be seen, with the increasing percentage of Al<sub>2</sub>O<sub>3</sub>, the behavior of the material against flame has improved. As the percentage of alumina increases, both the temperature rise slope behind the sample decreases, and at equal times, the temperature of the back of the sample with a higher percentage of alumina has a lower value and this difference is very significant. The temperature of the back of the insulation in the nanocomposite contains 8 w% of alumina (8ARC) is reduced by 521 °C compared to pure novolac resin (0ARC).

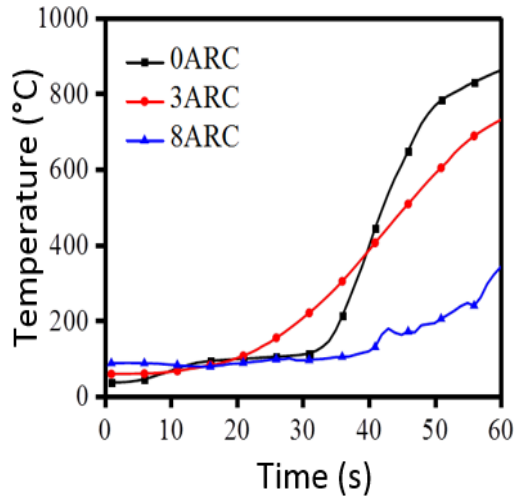


Fig 4. Temperature distribution of the back surface of 0ARC, 3ARC, and 8ARC nanocomposites, which were measured in OFT.

In the samples containing nano  $Al_2O_3$ , adding different percentages of nanoparticles has significantly improved the thermal properties, so that at the point of 20 seconds, the temperature behind the sample is 97, 77, and 35°C for 0ARC, 3ARC, and 8ARC, respectively. Therefore, the thermal properties of nanocomposite 8ARC have improved about three times compared to the control sample.

According to the ASTM E 285 standard, which is related to the oxyacetylene flame test method for insulations, one of the most important parameters for thermal insulations is the insulation index, which according to the following equation:

$$I_T = t_T/d$$

$I_T$  = insulation index at temperature  $T$ , s/m

$t_T$  = time for back-face temperature changes of specific temperature, s

$d$  = thickness of specimen, m

Where it measures the time, it takes for the temperature behind the sample to reach a certain and constant number, and therefore, the higher the index, the better the performance of the insulation.

Considering the temperature of 100°C as the index temperature, the insulation indexes for three samples, 0ARC, 3ARC, and 8ARC, are equal to 10500, 11500, and 21000 s  $m^{-1}$ , respectively. This indicates the increase in the insulating properties of the nanocomposite with the increase in the percentage of the presence of nanoparticles in the composite structure.

In addition, Figure 5 shows the image of the sample before and after the flame test.

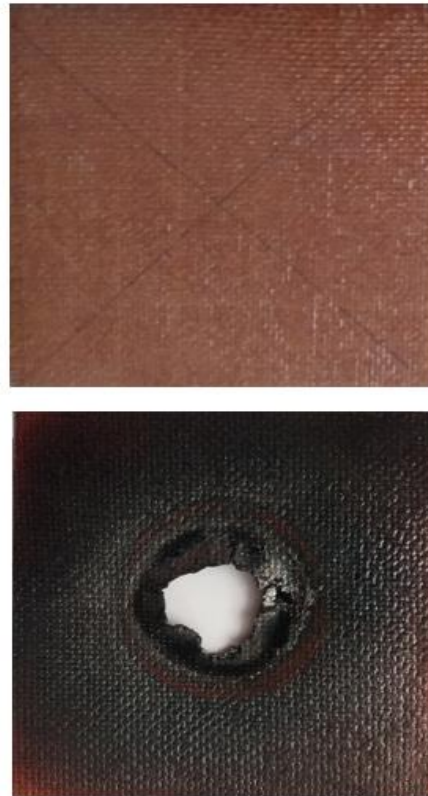


Fig 5. The sample image before and after OFT.

As the reason for improving the insulating properties of the composite by increasing the nanoparticles, it can be concluded that adding nanoparticles to the polymer structure affects its thermal properties in three ways: (1) absorption of heat through the change in the phase of nanoparticles from amorphous to crystal and then the aggregation of crystals and as a result, the transformation of nanoparticles into microparticles according to the latent heat of each of the mentioned steps; (2) increasing the heat dissipation by its reflection method, due to the increase in the effective surface of nanoparticles compared to microparticles; (3) thermal conductivity with change in particle size.

#### 4. Conclusion

In this research, alumina/novolac/fiberglass nanocomposites were synthesized by solution mixing at different nano alumina concentrations 3 (3ARC) and 8 w% (8ARC). SEM, EDS, and XRF were used to investigate the formation of nano alumina. According to SEM images, nanoparticles of  $Al_2O_3$  are uniformly dispersed in nanocomposites. Nevertheless, at higher weight percentages (8ARC), the aggregation of nanoparticles can occur. The EDS analysis confirmed the presence of alumina nanoparticles in 3ARC and 8ARC nanocomposites.

The XRF analysis data also showed that the nanocomposites are mainly composed of silicon in the form of silicon dioxide (related to the used fiberglass), which constitutes more than 35 w%. Also, based on the oxyacetylene flame test, thermal insulation properties of nanocomposites improve with increasing alumina content in nanocomposites, so that the insulation index at 100 °C for 0ARC, 3ARC, and 8ARC nanocomposites was 10500, 11500, and 21000 s m<sup>-1</sup>, respectively.

## Acknowledgment

The authors acknowledge the University of Zanjan for financial support.

## References

- [1] Ranade, R.A., Wunder, S.L. & Baran, G.R., 2006. Toughening of dimethacrylate resins by addition of ultra high molecular weight polyethylene (uhmwpe) particles. *Polymer*, 47 (12), pp.4318-4327.
- [2] Hirano, K. & Asami, M., 2013. Phenolic resins—100 years of progress and their future. *Reactive and Functional Polymers*, 73 (2), pp.256-269.
- [3] Pilato, L., 2013. Phenolic resins: 100 years and still going strong. *Reactive and Functional Polymers*, 73 (2), pp.270-277.
- [4] Guo, Z., Pereira, T., Choi, O., Wang, Y. & Hahn, H.T., 2006. Surface functionalized alumina nanoparticle filled polymeric nanocomposites with enhanced mechanical properties. *Journal of Materials Chemistry*, 16 (27), pp.2800-2808.
- [5] Tinghui, Y., 2001. Advance in the modifying research of high-performance phenolic resin. *Chemical Industry and Engineering Progress*, 20 (9), pp.13-16.
- [6] Zhang, W., Jiang, N., Zhang, T. & Li, T., 2020. Thermal stability and thermal degradation study of phenolic resin modified by cardanol. *Emerging Materials Research*, 9 (1), pp.180-185.
- [7] Johnsen, B., Kinloch, A., Mohammed, R., Taylor, A. & Sprenger, S., 2007. Toughening mechanisms of nanoparticle-modified epoxy polymers. *Polymer*, 48 (2), pp.530-541.
- [8] Suri, K., Annapoorni, S., Tandon, R. & Mehra, N., 2002. Nanocomposite of polypyrrole-iron oxide by simultaneous gelation and polymerization. *Synthetic Metals*, 126 (2-3), pp.137-142.
- [9] George, J. & Ishida, H., 2018. A review on the very high nanofiller-content nanocomposites: Their preparation methods and properties with high aspect ratio fillers. *Progress in Polymer Science*, 86, pp.1-39.
- [10] Ahmad, J. & Majid, K., 2020. Improved thermal stability metal oxide/go-based hybrid materials for enhanced anti-inflammatory and antioxidant activity. *Polymer Bulletin*, pp.1-23.
- [11] Mamunya, Y.P., Davydenko, V., Pissis, P. & Lebedev, E., 2002. Electrical and thermal conductivity of polymers filled with metal powders. *European polymer journal*, 38 (9), pp.1887-1897.
- [12] Wattanakul, K., Manuspiya, H. & Yanumet, N., 2010. The adsorption of cationic surfactants on bn surface: Its effects on the thermal conductivity and mechanical properties of bn-epoxy composite. *Colloids and Surfaces A: Physicochemical and Engineering Aspects*, 369 (1-3), pp.203-210.
- [13] Zhou, W., Qi, S., Li, H. & Shao, S., 2007. Study on insulating thermal conductive bn/hdpe composites. *Thermochimica Acta*, 452 (1), pp.36-42.
- [14] Sommers, A., Wang, Q., Han, X., T'joen, C., Park, Y. & Jacobi, A., 2010. Ceramics and ceramic matrix composites for heat exchangers in advanced thermal systems—a review. *Applied Thermal Engineering*, 30 (11-12), pp.1277-1291.
- [15] Wong, C. & Bollampally, R.S., 1999. Thermal conductivity, elastic modulus, and coefficient of thermal expansion of polymer composites filled with ceramic particles for electronic packaging. *Journal of applied polymer science*, 74 (14), pp.3396-3403.
- [16] Bazdar, H., Toghraie, D., Pourfattah, F., Akbari, O.A., Nguyen, H.M. & Asadi, A., 2020. Numerical investigation of turbulent flow and heat transfer of nanofluid inside a wavy microchannel with different wavelengths. *Journal of Thermal Analysis and Calorimetry*, 139 (3), pp.2365-2380.



- [17] Ruhani, B., Barnoon, P. & Toghraie, D., 2019. Statistical investigation for developing a new model for rheological behavior of silica-ethylene glycol/water hybrid newtonian nanofluid using experimental data. *Physica A: Statistical Mechanics and its Applications*, 525, pp.616-627.
- [18] Momohjimoh, I., Hussein, M.A. & Al-Aqeeli, N., 2019. Recent advances in the processing and properties of alumina-cnt/sic nanocomposites. *Nanomaterials*, 9 (1), pp.86.
- [19] Bahlawane, N. & Watanabe, T., 2000. New sol-gel route for the preparation of pure  $\alpha$ -alumina at 950° c. *Journal of the American Ceramic Society*, 83 (9), pp.2324-2326.
- [20] Mishra, A., Shukla, M., Shukla, M.K., Srivastava, D. & Nagpal, A.K., 2022. Thermal and mechanical characterization of alumina modified multifunctional novolac epoxy nanocomposites. *Polymers and Polymer Composites*, 30, pp.09673911221081827.
- [21] Yazman, Ş., Uyaner, M., Karabörk, F. & Akdemir, A., 2021. Effects of nano reinforcing/matrix interaction on chemical, thermal and mechanical properties of epoxy nanocomposites. *Journal of Composite Materials*, 55 (28), pp.4257-4272.
- [22] Mashayekhi, R., Khodabandeh, E., Akbari, O.A., Toghraie, D., Bahiraei, M. & Gholami, M., 2018. Cfd analysis of thermal and hydrodynamic characteristics of hybrid nanofluid in a new designed sinusoidal double-layered microchannel heat sink. *Journal of Thermal Analysis and Calorimetry*, 134 (3), pp.2305-2315.
- [23] Sarlak, R., Yousefzadeh, S., Akbari, O.A., Toghraie, D., Sarlak, S. & Assadi, F., 2017. The investigation of simultaneous heat transfer of water/al<sub>2</sub>o<sub>3</sub> nanofluid in a close enclosure by applying homogeneous magnetic field. *International Journal of Mechanical Sciences*, 133, pp.674-688.
- [24] Babu, B., Karthikeyan, P., Siva, K. & Sabarinathan, C., 2016. Study of erosion characteristics of mwcnt's-alumina hybrid epoxy nanocomposites under the influence of solid particles. *Digest Journal of Nanomaterials and Biostructures*, 11 (4), pp.1367-1373.
- [25] Baskaran, R., Sarojadevi, M. & Vijayakumar, C., 2011. Unsaturated polyester nanocomposites filled with nano alumina. *Journal of materials science*, 46 (14), pp.4864-4871.
- [26] Demircan, G., Kisa, M., Ozen, M. & Aktas, B., 2020. Surface-modified alumina nanoparticles-filled aramid fiber-reinforced epoxy nanocomposites: Preparation and mechanical properties. *Iranian Polymer Journal*, 29 (3), pp.253-264.
- [27] Ozen, M., Demircan, G., Kisa, M., Acikgoz, A., Ceyhan, G. & İşiker, Y., 2022. Thermal properties of surface-modified nano-al<sub>2</sub>o<sub>3</sub>/kevlar fiber/epoxy composites. *Materials Chemistry and Physics*, 278, pp.125689.
- [28] Demircan, G., Kisa, M., Ozen, M. & Acikgoz, A., 2021. Quasi-static penetration behavior of glass-fiber-reinforced epoxy nanocomposites. *Mechanics of Composite Materials*, 57 (4), pp.503-516.
- [29] Omrani, A., Simon, L.C. & Rostami, A.A., 2009. The effects of alumina nanoparticle on the properties of an epoxy resin system. *Materials Chemistry and Physics*, 114 (1), pp.145-150.
- [30] Derazkola, H.A. & Simchi, A., 2018. Effects of alumina nanoparticles on the microstructure, strength and wear resistance of poly (methyl methacrylate)-based nanocomposites prepared by friction stir processing. *Journal of the mechanical behavior of biomedical materials*, 79, pp.246-253.
- [31] Sengwa, R., Choudhary, S. & Dhatarwal, P., 2019. Investigation of alumina nanofiller impact on the structural and dielectric properties of peo/pmma blend matrix-based polymer nanocomposites. *Advanced Composites and Hybrid Materials*, 2 (1), pp.162-175.
- [32] Shukla, D.K., Kasisomayajula, S.V. & Parameswaran, V., 2008. Epoxy composites using functionalized alumina platelets as reinforcements. *Composites Science and Technology*, 68 (14), pp.3055-3063.
- [33] Kaybal, H.B., Ulus, H., Demir, O., Şahin, Ö.S. & Avcı, A., 2018. Effects of alumina nanoparticles on dynamic impact responses of carbon fiber reinforced epoxy matrix nanocomposites. *Engineering Science and Technology, an International Journal*, 21 (3), pp.399-407.

- [34] Azlin, M.N. & Zuraifah, M.S., 2013. Preparation and 3d morphology observation of phenolic resin-silica nanocomposites. *Growth*, 1, pp.2.